Seismic Retrofitting Effects of Reinforcing Over-Track Buildings with Knee-Brace Dampers

S. Yamada, K. Shimizu and Y. Takei
Railway Technical Research Institute, Japan

SUMMARY:
The study presented in this paper verifies the seismic retrofitting effects of reinforcing over-track buildings with knee-brace dampers. Firstly shaking table tests were carried out on large-scale test models, to simulate over-track buildings reinforced with knee-brace dampers. Resulting responses or hysteresis loops, confirmed the seismic retrofitting effects of knee-brace dampers. In addition, natural frequencies and damping factors of the models were estimated by ARX model. Furthermore, analytical study of over-track building models simulating true structures confirmed the seismic retrofitting effects of knee-brace dampers.

Keywords: over-track building, knee-brace damper, shaking table test, partial frame, ARX model

1. INTRODUCTION

Buildings spanning tracks (referred to below as over-track buildings) have structural characteristics such as high track story and no footing beams. Passing trains and passenger flow on the platform mean that placement of trackside earthquake-resisting elements such as braces and shear walls is difficult.

New over-track buildings are constructed in accordance with the Standard for Structural Design of Over-Track Low-Rise Buildings 2009 (RTRI, 2009) based on the Building Standard Law and seismic performance on the Design Standard for Railway Structures (Seismic Designs) (RTRI, 1999). Nonetheless, reinforcement of existing over-track buildings with dampers is important and useful. As incorporation of earthquake-resistant elements into over-track buildings is difficult due to limited space, the most commonly adopted dampers will be of knee-brace type. However, it is not easy to demonstrate the vibration-damping effect of knee-brace dampers due to the geometric relationship between the frame and the brace. In addition, there are few examples of studies on the effect of knee-brace dampers applied to steel-frame buildings (Koetaka et al., 2005 and Hasuda et al., 1998, 1999).

In view of the above, this study examined the seismic retrofitting effects of reinforcement of existing over-track buildings utilizing various kinds of knee-brace dampers. Shaking-table tests on large-scale samples confirmed a difference in damping effect and stresses on column-damper connections and beam-damper connections among various kinds of dampers. Moreover, an ARX (Auto-Regressive eXogenous) model (Adachi, 1993) was applied to estimate natural frequencies and damping ratios and evaluate the degree of variation in vibration characteristics. Finally, analytical studies of over-track building models simulating true structures, confirmed the seismic retrofitting effects of knee-brace dampers.

2. SHAKING TABLE TEST WITH PARTIAL FRAME

2.1. Outline of experiment

The main properties of the shaking table used in the trials are as follows: table size 7m in length and 5m in width; maximum loading capacity 50t; maximum acceleration, 2000cm/sec2; the maximum speed 150cm/sec; and maximum amplitude, 100cm.

In order to reduce the difference in behavior between the specimens and actual structures and taking into consideration various dependencies of damper the sample size should be as large as possible. However, the larger the sample, the larger the equipment ensuring the safety of the experiment has to be. In this experiment, the specimen was a 2/5 scale model of an actual track floor of an over-track building and represented the L-shaped part of the frame (beam measuring H-300x150x6.5x9, SS400 and column 200x200x9, BCP235) assuming building symmetry (Fig. 2.1). Pin type bearings were employed at the bases of column and the center of the beam. Inertial vibration excitation was applied to the specimens in the tests (Akiyama et al., 1998). The inertial force from the roller-supported mass (approximately 17 tons) acts through the natural rubber used for adjusting the first mode natural frequency. The estimated natural frequency of the frame utilizing white noise excitation (maximum acceleration 50 cm/sec2) is 1.47 Hz.

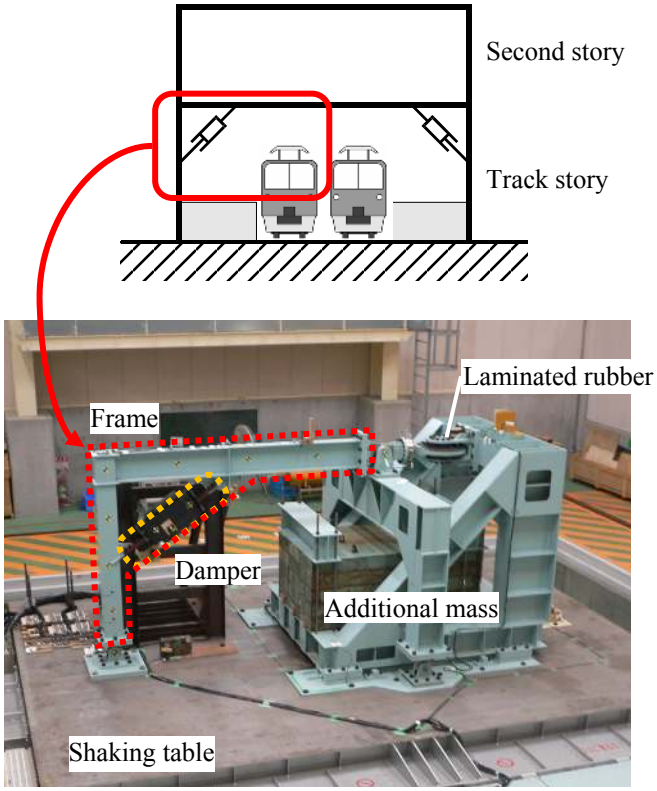

Figure 2.1. Overall view of the test rig

A damper is located at the corner of the frame (Fig. 2.1). This study investigated four kinds of damper: steel damper, viscoelastic damper, oil damper, and viscous damper with rotational inertia effect. The damper specifications were fixed so that the story deformation angle with damper reinforcement (hereafter referred to as ‘damper reinforcement’) equaled 1/100 at the input level for which the story deformation angle with no damper reinforcement (hereafter referred to as ‘no reinforcement’) equaled 1/50.

The damper connection plays an important role translating frame response to damper response. This study assumes the connection to be as shown in reference (Takei et al., 2000). Column-damper connections were welded at a slant and had a rib plate for restraining deformation of the column tube wall and buckling of the diaphragm. The beam-damper connection was also welded at a slant with a diaphragm adapted to the damper angle and fitted with a reinforcement rib (Fig. 2.2). All connecting materials are SM490 compliant.

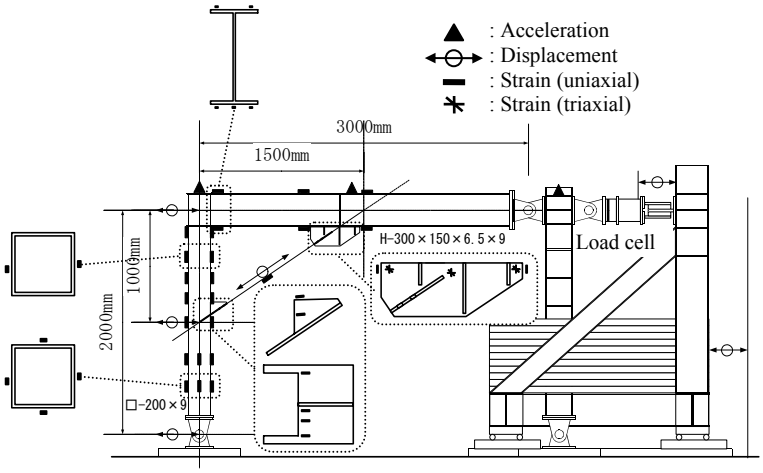

Figure 2.2. Main measurement points

Measurements were made for: acceleration, displacement, strain, load, and temperature. Fig. 2.2 shows the main measurement points. In addition, the axial force of the damper was calculated from the difference between shear forces of the upper and lower columns of the connection.

2.2. Vibration test procedure

The input earthquake motions were as follows: JMA Kobe-NS wave, Hachinohe-EW wave, the earthquake motion stipulated by the Building Standard Law (random phase, ordinary ground), and Level-2 earthquake motion (Spectrum II, G3 ground) set out in the Design Standard for Railway Structures (Seismic Designs) (RTRI, 1999). Table 2.1 shows the input levels. Levels A and B were determined by actual vibration responses without damper reinforcement of the frame. Levels C and D were 2.5 and 4.5 times greater than Level B respectively. In view of circumstances in terms of quantity of specimens, JMA Kobe-NS and Hachinohe-EW waves were applied for Level D.

Table 2.1. Input levels of earthquake motion

Level	Maximum story deformation angle without reinforcement	Earthquake motion
A	1/300	all
B	1/150	all
C	1/50	all
D	1/25	JMA Kobe-NS, Hachinohe-EW

The order of experiments was as follows: First Levels A and B were applied to the frame without damper reinforcement; subsequently the frame with damper reinforcement was subject to input Levels A, B, and C. Dampers were changed with the frame installed on the sliding table. Testing was pursued even when the frame seemed to have reached an area of slight plasticity. Then, Levels C and D were applied to the frame without damper reinforcement after having subjected it to Level D waves equipped with two kinds of dampers (viscous damper and viscoelastic damper). At this stage, the frame was replaced with a spare because the original sample had reached a state of large plastic deformation. The new frame without damper reinforcement was then tested with Levels A and B before being tested for Level D with the two remaining types of damper (oil damper and steel damper). Afterwards, Levels C and D were exerted onto the frame without damper reinforcement. White noise waves and impulse waves were applied to the frame as appropriate before and after inputting earthquake motion.

3. TEST RESULTS

3.1. Hysteresis loops

Fig. 3.1 shows the hysteresis loops of the various dampers under JMA Kobe-NS wave input Levels B and D. When level B was input, the steel damper did not yield and did not absorb energy. However, the other three kinds of damper with viscous systems, all absorbed energy. Hysteresis loops however took the form of large loops for all kinds of damper under Level D input and energy absorption was confirmed. The inertial mass demonstrated negative stiffness in the viscous damper. Although not shown here, the frame without damper reinforcement yielded significantly under Level D input, and displayed residual transformation (the maximum response relative story deformation was 91.3mm). On the other hand, relative story deformation decreased and there was no residual deformation when dampers were fitted.

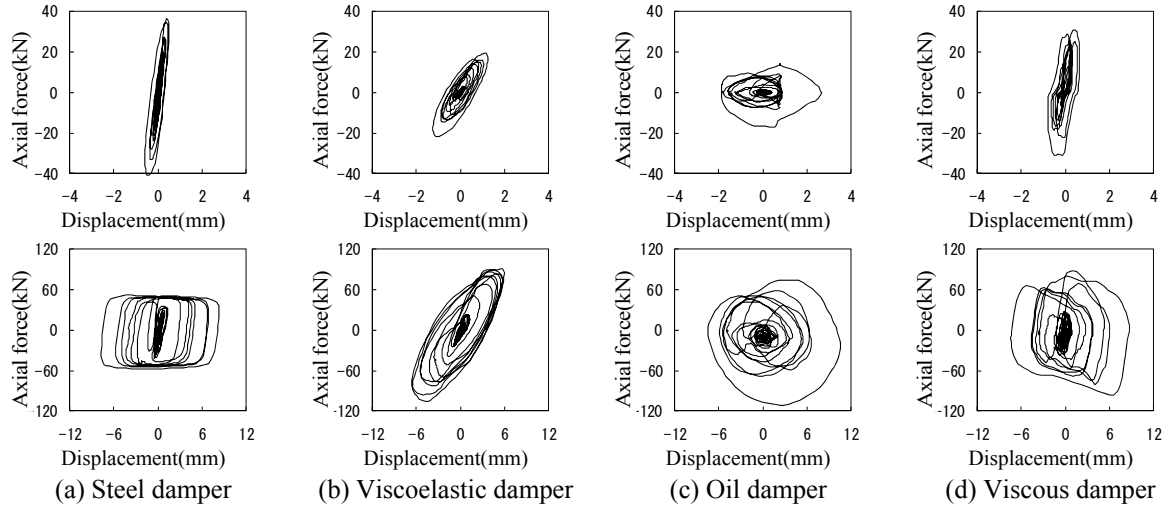

Figure 3.1. Hysteresis loops of various dampers under JMA Kobe-NS wave input
(the upper figure is for Level B and the lower figure is for level D)

3.2 Responses

Fig. 3.2 shows the averaged maximum absolute values of story deformation angles, beam accelerations, and shearing forces of the column bottom for each kind of damper and input level. The results in this figure are the ratios of the values obtained with damper reinforcement to those without reinforcement.

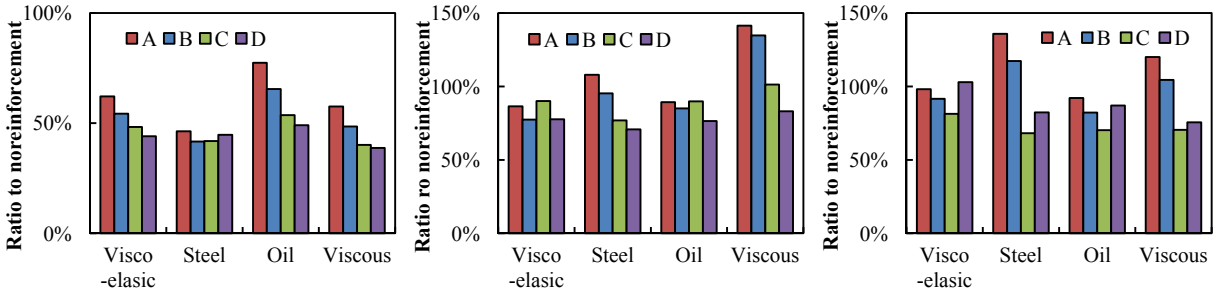

Figure 3.2. Maximum responses (ratio of values with damper reinforcement to no reinforcement
(for each type of damper)) (average values of four waves)

As the input level increased, the story deformation angles decreased for all dampers, and the effect of damper reinforcement grew as the input level rose. Given that the steel damper did not yield under Level B input, there was no reduction in response through energy absorption. However, it is presumed that the natural frequency was shortened by additional stiffness and responses decreased.

Accelerations and shearing forces were amplified under input Levels A and B in the case of both steel and viscous dampers. Additional stiffness is thought to be the cause of this in the case of the steel damper, and response amplification and additional stiffness in the case of the viscous damper. As input level grew, the effect of additional stiffness decreased relatively for both kinds of damper, and response amplification disappeared. For the steel damper, this is due to a decrease in additional stiffness as the damper yielded, whereas for the viscous damper, this is caused by falling inclination of the load-velocity curve and the effect of negative stiffness due to inertial mass. The rate of response reduction of shearing forces tended to be lower under Level D input than Level C input. It was presumed that it is difficult to raise the shearing force because the frame without damper reinforcement reaches a plastic state under Level D input.

3.3 Strain

Fig. 3.3 shows the maximum strain of the frame under JMA Kobe-NS wave Level D input. Even without reinforcement, connection parts were installed on the beam and the column.

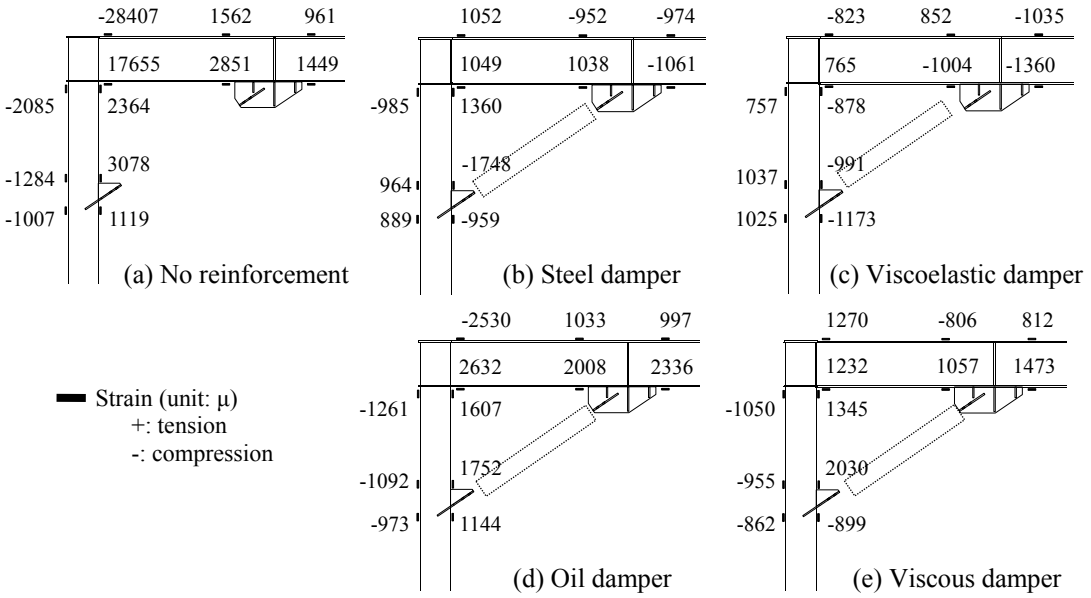

Figure 3.3. Maximum strain of frame under JMA Kobe-NS wave input of Level D

In the case of the frame without damper reinforcement, the maximum value was -28407μ at the upper surface of the beam at the beam-column connection. In this case, the residual deformation of the frame remained and beam paint peeled off. In all the cases where the frame had damper reinforcement, the strain on the beam-column connection fell, and the maximum value recorded overall was 2632 μ on the lower surface of the beam at the beam-column connecting interface. In the case of the frame with damper reinforcement, maximum strain values did not seem to occur with any particular regularity and were of the same magnitude at respective connections. Based upon the above, it was confirmed that the strain concentrated at the beam-column connection of the frame dispersed and generally decreased due to damper reinforcement.

Moreover, the maximum damper-connection strain value was -1337μ at the rib plate for preventing buckling of diaphragm of column-damper connection. It was confirmed that the key member, responsible for transmission of power between the damper and the frame, did not yield earlier than the

frame.

3.4 Vibration characteristics

3.4.1 Evaluation method

Vibration characteristics were estimated utilizing an ARX model. The input is acceleration on the shaking table and the output is acceleration on the beam. The ARX model had a degree of 10 and input and output filters band pass filter of 0.3-3.0Hz.

Tables 3.1 and 3.2 show the averaged damper ratios and the natural frequencies by type of damper and input level, respectively. Fig. 3.4 shows the ratio of natural frequencies between cases with damper reinforcement and cases without. In consideration of the natural period for lengthening of the frame through plasticization under Level C or D inputs, the average of the natural frequencies under input Levels A and B were adopted as the values in the case where there was no reinforcement. Fig. 3.5 illustrates differences in damping ratio for cases with damper reinforcement and cases without. Since there was variation of influences such as friction damping of bearing units according to input level, the damping ratios in the case of no reinforcement were adopted as the value estimated under each input level. However, the damping ratio under Level C input was employed as the value for Level D input because of hysteretic damping by plasticization of the frame increased under Level D input.

Table 3.1. Natural frequencies (Hz)

Dampers	A	B	C	D
No reinforcement	1.39	1.38	1.32	1.30
Steel damper	1.95	1.91	1.80	1.67
Viscoelastic damper	1.77	1.73	1.62	1.60
Oil damper	1.54	1.50	1.47	1.46
Viscous damper	1.85	1.85	1.82	1.66

Table 3.2. Damping ratios

Dampers	A	B	C	D
No reinforcement	0.09	0.09	0.04	0.06
Steel damper	0.08	0.06	0.10	0.11
Viscoelastic damper	0.15	0.14	0.10	0.09
Oil damper	0.21	0.20	0.20	0.19
Viscous damper	0.11	0.11	0.16	0.19

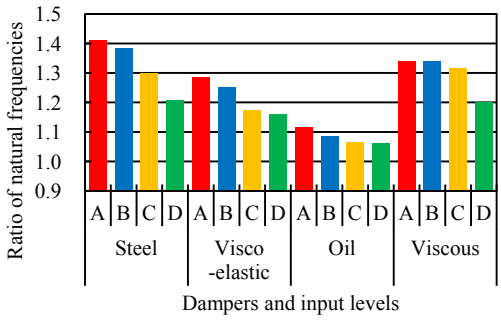

Figure 3.4. Ratio of Natural frequencies (damper reinforcement / no reinforcement)

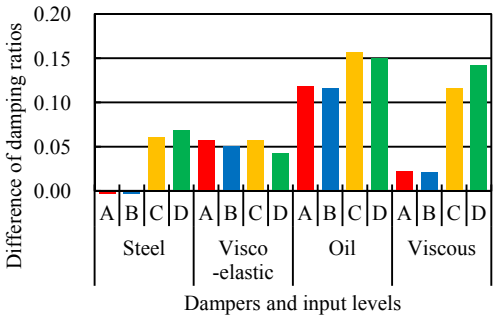

Figure 3.5. Difference in damping ratios (damper reinforcement - no reinforcement)

3.4.2 Natural frequencies

In the case of the steel damper, natural frequency increased the most under Level A input and remained at almost the same value under Level B input for which the damper was approximately in the elastic range. However, under the Levels C or D input, it decreased and the steel damper yielded. In the case of the viscous damper, influence of additional stiffness by the response amplification was significant, accordingly there was a large increase in natural frequency under Levels A, B, and C input. For Level D input however, it decreased due to a fall in the inclination of the load-velocity curve and negative stiffness due to inertial mass. For the viscoelastic and oil dampers, ratios grew as input levels fell.

3.4.3 Damping ratios

As shown in Table 3.2, the damping ratios without reinforcement are around 9%, 4%, and 6% for level

A and B, level C, level D input respectively. The damping due to roller bearings, pin bearings, and the laminated rubber is incorporated into these damping ratios. Because the laminated rubber behavior was approximately elastic in all the experimental scenarios, it is considered that the additional damping due to the laminated rubber is constant regardless of input level. Therefore, it is thought that damping ratios under Levels A and B input were largely influenced by the friction damping in bearings. In addition, damping ratios generally decreased, as input levels grew. On the other hand, plasticization in the case of Level D input added hysteretic damping to the frame. As for the steel damper, 5% of additional damping was observed after the steel damper yielded. Additional damping was identified as being approximately constant regardless of the input level in the case of the viscoelastic and oil dampers. The values were just over 10% for the oil damper and around 5% for the viscoelastic damper. In the case of the viscous damper, additional damping under Levels A and B input was around several percent, however, it suddenly increased under Levels C and D input and additional damping of more than 10% was observed.

4. ANALYTICAL VERIFICATION OF TEST RESULTS

4.1 Analytical models and conditions

Analytical verification was made of test results obtained for the steel and oil dampers. The analysis model only modeled the frame in the form of beam elements. All jigs were modeled except for dummy elements on the frame with very large stiffness and yield strength whose mass was concentrated together at the nodes. The laminated rubber for adjusting the natural period with quasi-elastic behavior was modeled with the stiffness of an elastic spring, which was determined by linear approximation of the load-deformation curve for laminated rubber. Pin bearings were modeled in spite of physical size, and the frictional resistance of roller bearings was considered as a bilinear model. The damper specifications were revised using test results and design values with due consideration on the influence of the damper connections. In addition, in the frame comprising the knee-brace damper set up, deformation of damper connections was expected to influence frame response. Two scenarios were considered for setting the rigid zone (Fig. 4.1): one option was to set the rigid zone only at the column-beam connection, and the other was to set it at both the column-beam connection and at the damper connection. Earthquake input motion was supplied by acceleration of the shaking table in the test. Damping was assumed as proportional to the strain energy on the members.

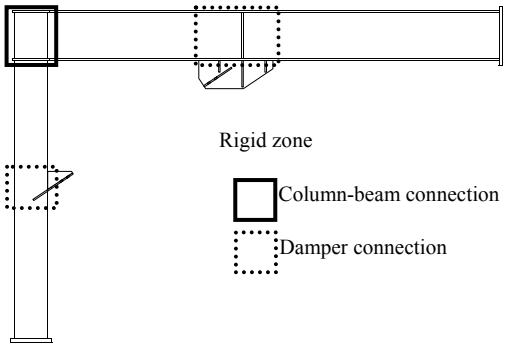

Figure 4.1. Rigid zone

4.2 Eigenvalue analysis

Table 4.1 shows natural frequencies, damping ratios and effective mass in the absence of reinforcement. The frame and additional mass work in the same direction with in the first mode, which is a very dominant mode where the effective mass ratio exceeds 99%. In the second mode the frame and additional mass worked in the reverse phase. The natural frequency of the first mode was 1.46Hz and almost agreed with the estimated value from the preliminary experiment.

Table 4.1. Results of Eigenvalue analysis

Modes	Natural frequency (Hz)	Damping ratio	Effective mass (%)
First	1.46	0.02	99.63
Second	14.88	0.01	0.33

4.3 Response analysis

Fig. 4.2 shows time histories of response for story deformation under JMA Kobe-NS Level C wave input. The residual deformation observed in steel damper tests could not be reproduced regardless of rigid zones being set. Excluding this however, the validity of the modeling was confirmed because the result reproduced almost exactly the shape and response values of time histories for both the dampers. The responses of the model without set rigid zones were larger than the model with set rigid zones, although the difference was small.

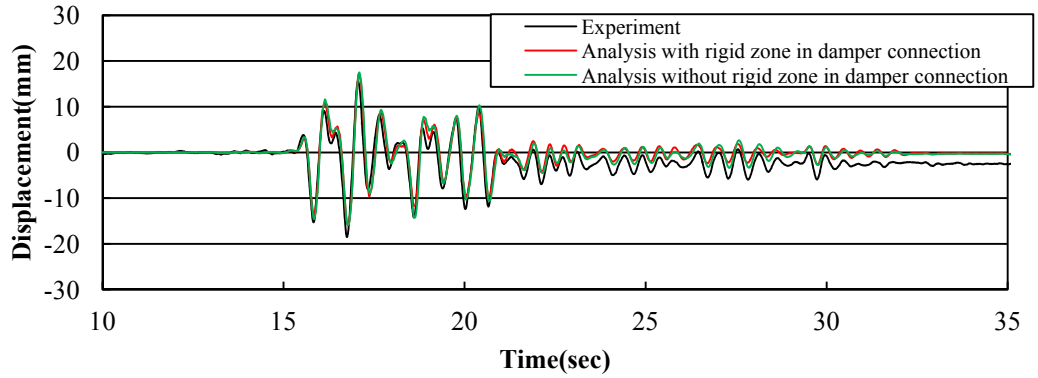

(a) Steel damper

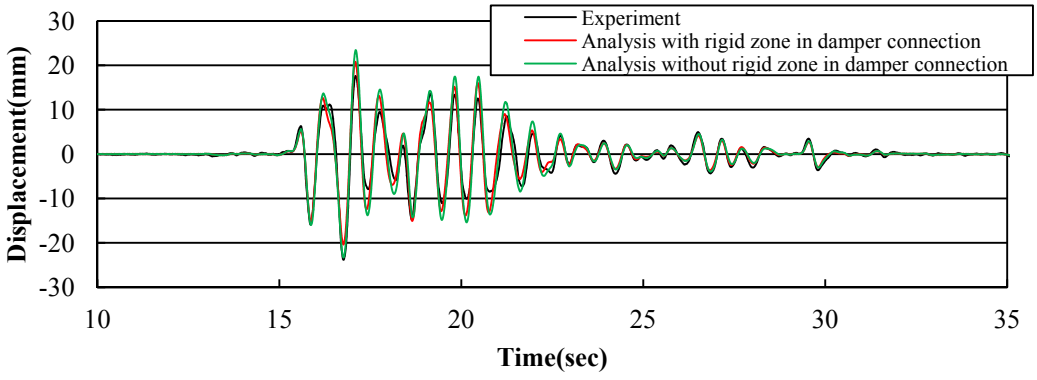

(b) Oil damper

Figure 4.2. Time history of response relative story deformation

5. ANALYTICAL STUDY OF OVER-TRACK BUILDINGS USING MODEL SIMULATION

The behavior of damper reinforced over-track buildings was subject to analysis by adopting steel and oil damper parameters as the damper specifications. The analysis model was of an over-track building with two-stories and one-span. No rigid zone was set in this case at the damper connections.

5.1 Analysis model

The model applied for analysis was a two-dimensional frame model with an earthquake resistance performance as stipulated in the Standard for Structural Design of Over-Track Low-Rise Buildings 1987 (RTRI, 1987). Fig. 5.1 shows the shape and specifications of the model.

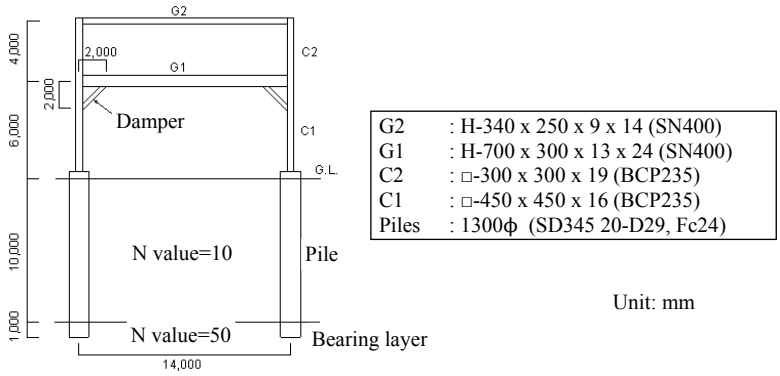

Figure 5.1. Analysis model

The earthquake resistance performance of this model was set below the earthquake resistance performance of the current standard (RTRI, 2009), and the response deformation (1/25) exceeded the deformation capacity (1/36) under Level-2 earthquake motion (Spectrum II, G3 ground) stipulated by the Design Standard for Railway Structure (Seismic Designs). The ratio of horizontal load bearing capacity (Qu) to the necessary horizontal load bearing capacity (Qun) was Qu/Qun=1.09 under the current standard rule; although this rate satisfies the rule, the margin is small.

Table 5.1 shows the damping ratio and hysteretic characteristics of members. Level-2 earthquake motion (Spectrum II, G3 ground) stipulated by the Design Standard for Railway Structure (Seismic Designs) was applied as the input earthquake motion. In addition, the earthquake motion was input at the same time without considering phase differences between ground springs. Damper specifications were determined through trial and error, adopting first stiffness and yield resistance as parameter for the steel damper, and relief velocity and relief load for the oil damper. The dampers were installed 2m away from each column-beam connection corner as shown in Fig. 5.1.

Table 5.1. Analytical condition

Members	Hysteretic characteristic	Damping Ratio
Horizontal ground spring	Normal bilinear	0.10
Steel	Normal bilinear	0.02
Reinforced Concrete	Takeda	0.03

5.2 Analysis results

The responses were evaluated by the ratio of values with damper reinforcement to values in the absence of reinforcement. As for the story deformation angles of the track floor, the ratio decreased to around 0.6 with the oil damper and around 0.7 with the steel damper. However, with story shear forces and response acceleration of the track floor, the ratio increased to around 1.3 and around 1.2 respectively for both dampers. These tendencies were similar to those of the test results. In addition, all responses tended to increase on the second floor, which was not reinforced.

Fig. 5.2 shows the plastic hinge outbreak points and cumulative plastic strain energy. Plastic hinges concentrated at the column-beam connections dispersed, and cumulative plastic strain energy implying damage of the frame decreased. The maximum bending moment of piles increased to around 1.18 times for both dampers compared to when reinforcement was not used (1700kNm). The flexural strength of piles assumed in these analysis examples was approximately 2500 kNm when there was no axial force. Tension axial forces were not generated in the piles. Accordingly, this confirmed that piles were less likely to be damaged.

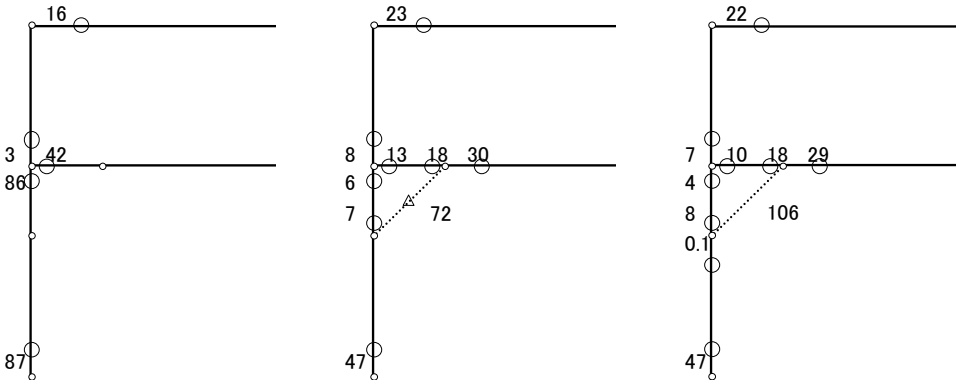

(a) No reinforcement (b) Steel damper (c) Oil damper

Figure 5.2. Plastic hinge outbreak point (Values are cumulative plastic strain energy, unit: kNm)

6. CONCLUSION

Verification was made of seismic reinforcement effects of over-track buildings with knee-brace dampers through experiment and analysis.

1. Shaking table tests with a partial frame, representing the over-track building, confirmed the effects of dampers and the stress conditions at the beam-column, column-damper, and beam-damper connection points, respectively.
2. Natural frequency and damping ratio were estimated in tests utilizing the ARX model and changes under different input levels and kinds of dampers were evaluated.
3. It was possible to reproduce test results by modeling the frame using beam elements.
4. The over-track building was analyzed using model simulating true structure and the influence of damper reinforcement on piles, which are not able to be reinforced, was investigated.

This paper has discussed seismic reinforcement of over-track buildings. It has found out that the system using knee-brace dampers are also applicable to new constructions. In future, it is hoped that this system will be incorporated into the rational design of the over-track buildings.

REFERENCES

Railway Technical Research Institute (RTRI), ed. (2009). Standard for Structural Design of Over-Track Low-Rise Buildings 2009, Association of Railway Architects, JAPAN (in Japanese).

Railway Technical Research Institute (RTRI), ed. (1999). Design Standard for Railway Structure (Seismic Designs), Maruzen, JAPAN (in Japanese).

Koetaka, Y., Ando, M., Byakuno, Y., Suita, K., and Inoue, K. (2005). Full-Scale Test of Weld-Free Steel Structure with Knee Brace Dampers. *Journal of Structural and Construction Engineering*. **No.595**, 109-116 (in Japanese).

Hasuda, T., Takada, K., Ishibashi, T., Ichinohe Y., Takei, Y., Hirayama, H., Fukuda, K., Yam, M., Kubota, K., and Osako, K. (1998,1999). Seismic Retrofit of Over-Track Buildings Using Brace-Type Hysteretic Dampers, Parts 1 to 6. *Summaries of Technical Papers of Annual Meeting*. **B2**, 911-918, 1998 / 901-904 (in Japanese).

Adachi, S. (1993). Theory of System Identification for the User. Corona Publishing, JAPAN (in Japanese).

Akiyama, H., Yamada S., Minowa C., Teramoto T., Otake F., Yabe Y. (1998). Experimental Method of the Full Scale Shaking Table Test Using the Inertial Loading Equipment. *Journal of Structural and Construction Engineering*. **No.505**, 139-146 (in Japanese).

Takei, Y., Takada, K., Hasuda, T., Ichinohe Y., Ishibashi, T., Fukuda, K., Hirayama, H. (2000). Seismic Retrofit of Over-Track Buildings Using Brace-Type Hysteretic Dampers, Parts 7 and 8. *Summaries of Technical Papers of Annual Meeting*. **C1**, 973-976 (in Japanese).

Railway Technical Research Institute (RTRI), ed. (1987). Standard for Structural Design of Over-Track Low-Rise Buildings 1987, Association of Railway Architects, JAPAN (in Japanese).